Effect of Ni^{2+} as a Codopant on the Structure, Morphology, and Conductivity of Nanostructured Polyaniline

Man Jiang, Shibu Zhu, Zuowan Zhou, An Zhao, Jun Lu

Key Laboratory of Advanced Technologies of Materials, Ministry of Education, School of Materials Science and Engineering, Southwest Jiaotong University, Chengdu 610031, People's Republic of China

Received 26 April 2010; accepted 7 December 2010
DOI 10.1002/app.33867
Published online 12 April 2011 in Wiley Online Library (wileyonlinelibrary.com).

ABSTRACT: One-dimensional nanostructures of polyaniline (PANI) doped with (1S)-(+)-10-camphorsulfonic acid (D-CSA) alone and with $NiCl_2$ as a codopant were synthesized via *in situ* polymerization. PANI nanofibers with diameters of about 200 nm were formed when PANI was doped with D-CSA only. When $NiCl_2$ was added as a codopant, the morphology of PANI obviously changed. The effects and related mechanisms were investigated by Fourier transform infrared spectroscopy, ultraviolet–visible spectroscopy, inductively coupled plasma–atomic emission spectroscopy, and X-ray diffraction, and the results indicated that Ni^{2+} destroyed the micelles' structure by chemical conjunction with $-SO_3H$ groups in camphorsulfonic acid (CSA) molecules, which were the key component in forming the CSA–aniline micelles. The combination between Ni^{2+} and SO_3^- in CSA with a lower addition of Ni^{2+} led to a reduction of CSA doping to PANI, but a higher loading of Ni^{2+} brought about the direct doping of Ni^{2+} to PANI, which caused a higher degree of doping and oxidation. The conductivity of PANI increased almost linearly with increasing Ni^{2+}. © 2011 Wiley Periodicals, Inc. J Appl Polym Sci 121: 3439–3445, 2011

Key words: infrared spectroscopy; 'microstructure; polymer synthesis and characterization

INTRODUCTION

As a conducting polymer, polyaniline (PANI) has attracted more and more attention because of its chemical stability, adjustable conductivity, controllable structures, and abundant morphologies.[1] Enlightened by the success of carbon nanotubes[2] and other nanostructured semiconductors,[3] researchers have given a great deal of attention to the one-dimensional (1-D) nanostructures of PANI, such as nanotubes,[4] nanofibers,[5] nanowires,[6] and even molecular wires,[7] because of their promising potential applications in both nanotechnology and polymer science. With regard to the approaches for preparing low-dimensional PANI, they can generally be categorized into template processes[8] and template-free methods[9] according to whether an exterior template is used or not. By comparison, the latter, also called *soft-template methods*, which form by micellar structures, has been the subject of more studies because of its simple procedures, easy controllability, low cost, and, what is more, academic challenges for revealing the mechanisms or the genesis. Generally, almost all of the template-free assembled 1-D nanostructures of PANI have been obtained by *in situ* polymerization, in which the dopant governed not only the molecular structures but also the morphologies and physical properties of the polymers as well.[10] The use of metallic ions as a codopant in *in situ* polymerization has also captured the attention of researchers. Sengupta et al.[11] used Li^+ as a codopant during the polymerization of aniline (Ani) to improve the electrical properties of PANI, and the result indicates that the presence of Li^+ ion acted as an instantaneous site of nucleation and led to larger chain growth and resonance stabilization. Hydrochloric acid has commonly been used as an effective dopant for the chemical synthesis of PANI nanofibers and nanowires.[12] Zhang et al.[13] added several kinds of inorganic salts, such as LiCl, NaCl, $MgCl_2$, or $AlCl_3$, as additives in the system of HCl-doped *in situ* polymerization, and a series of chrysanthemum flowerlike microstructures were obtained by self-assembly. In general, alkali-metal or alkaline-earth-metal ions, such as Li^+, Na^+, and Mg^{2+}, have great effects on the morphology of PANI. The transition metals, however, have an unfilled *d* orbital, and their properties are quite different from those of other metals. Understanding the interactions between the transition-metal ion and the conjugated

Correspondence to: Z. Zhou (zwzhou@at-c.net).
Contract grant sponsor: National Natural Science Foundation of China; contract grant number: 90305003.
Contract grant sponsor: Special Research Fund for the Doctoral Program of Higher Education; contract grant number: 20060613004.
Contract grant sponsor: National Hi-Tech (863) Program of China; contract grant number: 2008AA030705.

chain of PANI are essential for both the theoretical and application points of view. Yang and Chen[14] reported that PANI containing transition-metal ions, such as Fe^{3+}, Co^{2+}, Ni^{2+}, and Cu^{2+}, had greatly different structures from those of emeraldine base (EB)- or HCl-doped PANI. To the best of our knowledge, there have been few studies[14–16] on PANI nanostructures doped with Ni^{2+}; however, there have been no reports on the characteristics of PANI with acid and Ni^{2+} as codopants. It may be of importance to confirm whether the transition-metal ion Ni^{2+} could be chemically doped onto the molecular chains of a conducting polymer and result in a magnetic polymer. In this article, we report the effects and related mechanisms of $NiCl_2$ as a codopant with (1S)-(+)-10-camphorsulfonic acid (D-CSA) for *in situ* polymerization on the structures, morphologies, and electrical properties of PANI with low-dimensional nanostructures. The results may be promising for the preparation of new functional polymers, such as organic magnets based on metallic-ion-doping conducting polymers.

EXPERIMENTAL

Materials

Ani was distilled under reduced pressure and stored below 0°C. Ammonium peroxydisulfate [APS; $(NH_4)_2S_2O_8$], $NiCl_2{\cdot}4H_2O$, and D-CSA were all of analytical purity and were used without further purification, and all of the experiments were carried out with deionized water.

Polymerization

Ani (0.002 mol) and D-CSA (0.001 mol) were dissolved in 20 mL of deionized water under mechanical stirring for 10 min to form a uniform solution. A 10-mL aqueous solution of $NiCl_2$ (specific molar quality) and a 20-mL aqueous solution of APS (0.002 mol) were then added to the previous solution in turn. Then, the previous mixture continued to polymerize under static conditions at 0–5°C for 16 h. The obtained dark green precipitate was washed with deionized water and ethanol several times. The product was dried *in vacuo* at about 60°C for 24 h. To investigate the effect of Ni^{2+} on the product, the $[NiCl_2]$/[Ani] molar ratios in the polymerization system were varied as 0, 0.5, 1.0, and 2.0 with the [camphorsulfonic acid (CSA)]/[Ani] and [APS]/[Ani] ratios fixed at 0.5 and 1.0, respectively.

Structural characterizations

Fourier transform infrared (FTIR) spectra (KBr dispersed pellets) in the range 400–4000 cm^{-1} were recorded on a fully computerized Nicolet 5700 spectrometer (Madison, Wisconsin, USA) at a resolution of 4 cm^{-1}. The ultraviolet–visible (UV–vis) absorption spectra were obtained on a UV-2550 UV–vis spectrophotometer (Shimadzu, Japan). The X-ray diffraction (XRD) patterns were recorded on a Philips X'Pert PRO X-ray diffractometer (Cu Kα radiation). The morphologies of the samples were observed on a Quanta200 scanning electron microscope and a Quanta200 H-700H Hitachi transmission electron microscope. Before the scanning electron microscopy (SEM) characterization, all of the samples were coated with gold. The amount of nickel element in the resulting PANI was analyzed by inductively coupled plasma–atomic emission spectroscopy (ICP–AES; Thermo Jarrell Ash, ICPS-1000). The electrical conductivities of the pressed pellets at room temperature were measured by a standard four-probe method on an SZ82 digital instrument.

RESULTS AND DISCUSSION

Morphological observations

Figure 1 gives the SEM and transmission electron microscopy images of the CSA–Ni^{2+} co-doped PANI with different molar ratios of $[NiCl_2]$ to [Ani]. To determine the effect of inorganic salts on the morphology of PANI nanofibers, we synthesized PANI without and with $NiCl_2$ as the additive. As shown in Figure 1, the well-distributed nanofibers had diameters of about 200 nm and lengths of around several micrometers with D-CSA as the only dopant. With increasing dosage of $NiCl_2$ in the polymerization system, the nanofibers were inclined to become shorter and shorter and finally form nanoparticles. As shown in Figure 1(b), the length of PANI nanofibers got shorter and the morphology turned to a network instead of well-distributed nanofibers when the molar ratio of $[NiCl_2]$ to [Ani] was 0.5. As the ratio went up to 1 or 2, moreover, there was no nanofiber formed in the precipitate, but only nanoparticles could be found in the product [Fig. 1(c,d)].

As described previously, the morphology of the PANI was affected by the molar ratio of $[NiCl_2]$ to [Ani] in the reaction system. The micelles, consisting of D-CSA anion and anilinium cation before polymerization, acted as a templates in the formation of PANI–(D-CSA) nanofibers.[17] When the $NiCl_2$ was added, however, Ni^{2+} destroyed the D-CSA/Ani micelles by interaction between Ni^{2+} and SO_3^-. Thus, it might have affected the morphology of PANI when the Ni^{2+} was used as a codopant; this is discussed in the following section.

Detailed explanations to the effect of Ni^{2+} on the structure and morphology of nanostructured PANI

To understand the related mechanism for the effect of Ni^{2+} on the morphology of the nanostructures of

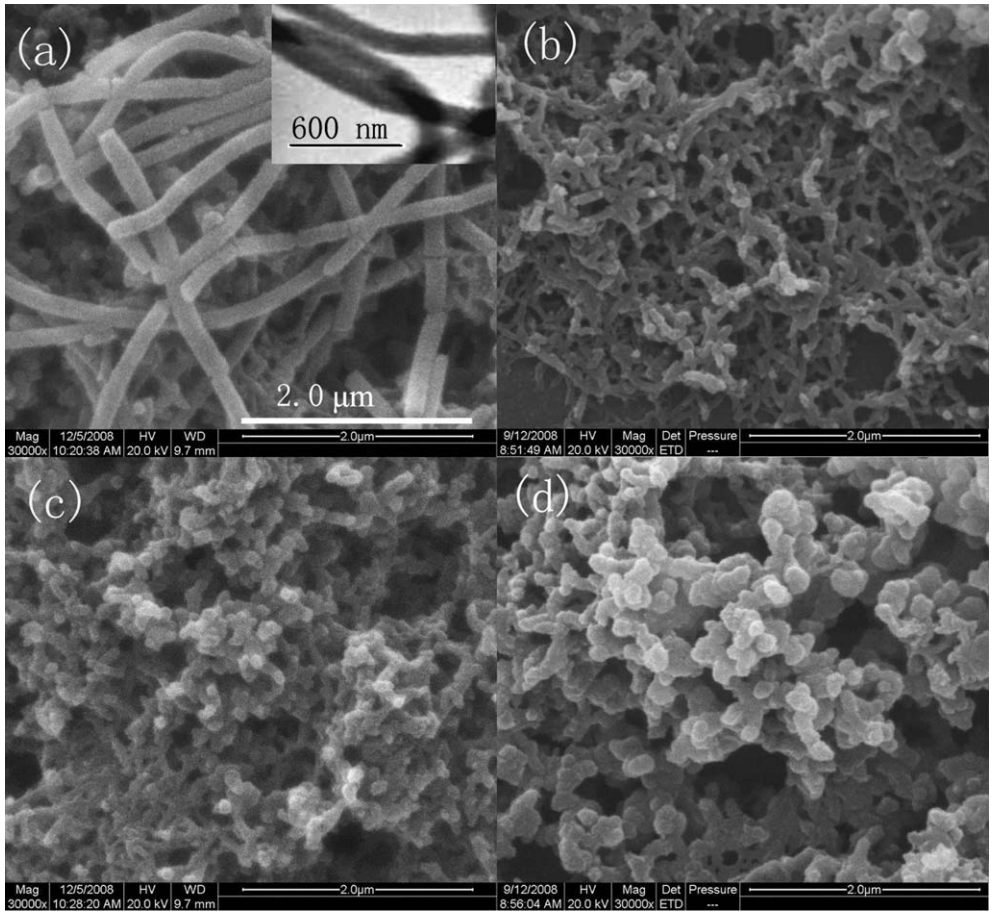

Figure 1 SEM images of the PANI prepared at molar ratios of $NiCl_2$ to Ani: (a) 0, (b) 0.5, (c) 1.0, and (d) 2.0. The inset transmission electron microscopy image in photo a indicates that it was a solid fiber.

PANI, we analyzed the FTIR spectra of the Ani–CSA and Ani–CSA–Ni^{2+} compounds before polymerization. As shown in Figure 2, in which curves a, b, c, and d correspond to the IR spectra of Ani, CSA, Ani–CSA, and Ani–CSA–$NiCl_2$ ([Ani]/[$NiCl_2$] = 1.0), respectively, the typical peaks of Ani and CSA, such as the stretching vibrations of N—H (3413 cm^{-1}), O—H (3433 cm^{-1}), and C—H (2920–2960 cm^{-1}), were obvious in curves a and b. For the compound Ani–CSA, the C=O stretching vibrations in CSA molecules (1740 cm^{-1}), the S—O asymmetry stretching vibration (1185 cm^{-1}),[18,19] the C—S stretching vibration (746 cm^{-1}), and the S—O stretching vibration (616 cm^{-1})[20,21] were still observed, but the stretching vibration at about 3440 cm^{-1} for N—H or O—H was much weaker than those of Ani or CSA alone, and a new strong peak at 2637 cm^{-1} emerged. This could be ascribed to the stretching vibrations of N—H in the primary ammonium ion (as shown in Fig. 3).[22] From this, we suggest that a chemical reaction of —NH in Ani and —SO_3H in CSA took place and formed the micelle of the Ani–CSA compound. In curve d, for the compound Ani–CSA–Ni^{2+} ([Ani]/[Ni^{2+}] = 1.0), the stretching vibrations for N—H and O—H resumed at about 3430 cm^{-1}, whereas the conjunction peak at 2637 cm^{-1} disappeared. On the basis of this result, we put forward a schematic explanation for the mechanism of effect of Ni^{2+} on

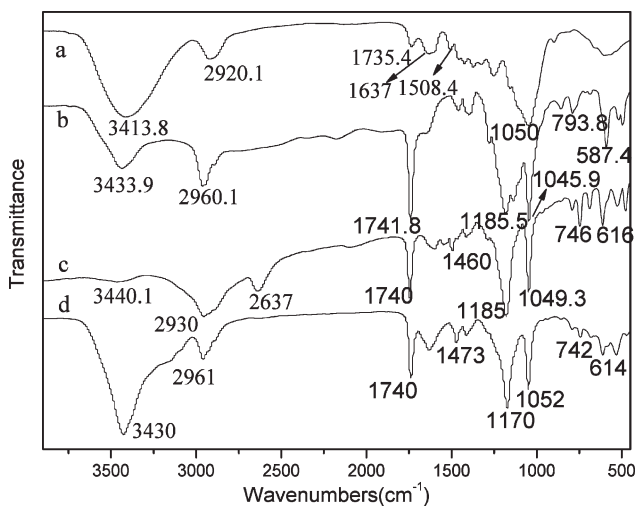

Figure 2 FTIR spectra related to (a) Ani, (b) CSA, (c) Ani–CSA, and (d) Ani–CSA–$NiCl_2$ ([Ani]/[Ni^{2+}] = 1.0).

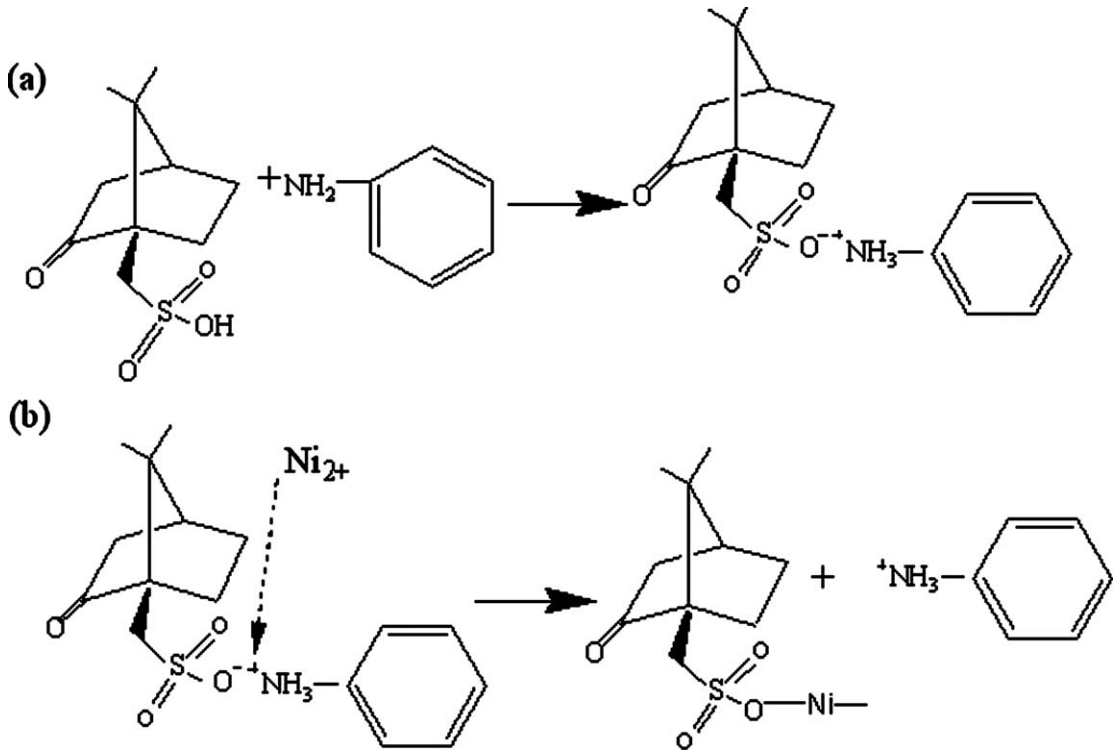

Figure 3 Schematic for the (a) formation of micelles composed of CSA and Ani and (b) formation of the Ni—SO_3 compound.

the micelle. Generally, the Ani–CSA micelles were formed by chemical combination between the —NH and —SO_3H groups. With the addition of Ni^{2+}, as indicated in Figure 3(b), a new reaction between the Ni^{2+} and —SO_3H group replaced the former conjunction of —NH and —SO_3H and led to the dissociation of the micelles. As a result, the N—H stretching vibration recovered, and because of the Ni^{2+} restraint, the S—O asymmetry stretching vibration in the SO_3^- group shifted from 1185 to 1170 cm^{-1}, and the C—H stretching vibration shifted from 1460 to 1473 cm^{-1}. Figure 4, in which curves a, b, c, and d represent the samples with [$NiCl_2$]/[Ani] molar ratios of 0, 0.5, 1.0, and 2.0, respectively, shows the FTIR spectra of the Ani–CSA–$NiCl_2$ compounds. With increasing Ni^{2+}, the strength of the N—H stretching vibration (3440 cm^{-1}) was enhanced, and the conjunction absorption at 2637 cm^{-1} disappeared. This phenomenon was ascribed to the dissociation of Ani from the Ani–CSA micelles. Furthermore, a shoulder peak at about 3100 cm^{-1} on curves c and d in Figure 4 became more and more noticeable; this may have resulted from stronger and stronger conjunctions between Ni^{2+} and SO_3^-.

As is well known, nanostructured PANI is governed by the micelles formed by Ani and CSA. It was reasonable to speculate that Ni^{2+} influenced the morphology of the nanostructured PANI by affecting the structures of the micelles. Figure 5 shows the FTIR spectra of PANI doped with D-CSA alone and with $NiCl_2$ as a codopant at different molar ratios of [$NiCl_2$] to [Ani]. In all of the samples, the characteristic vibrations of PANI, such as the C=C stretching vibration of the quinoid ring at about 1578 cm^{-1} and that of the benzene ring at 1500 cm^{-1},[23] the C—N stretching of secondary aromatic amine at 1300 cm^{-1}, the aromatic C—H in-plane band at

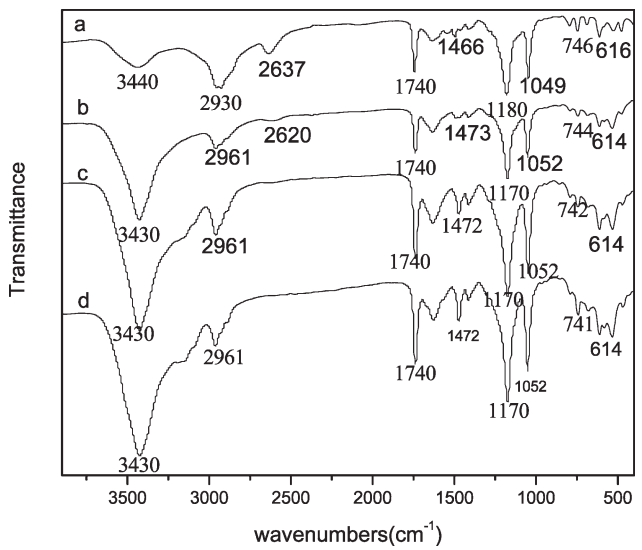

Figure 4 FTIR spectra of the Ani–CSA–$NiCl_2$ compounds with [$NiCl_2$]/[Ani] molar ratios of (a) 0, (b) 0.5, (c) 1.0, and (d) 2.0.

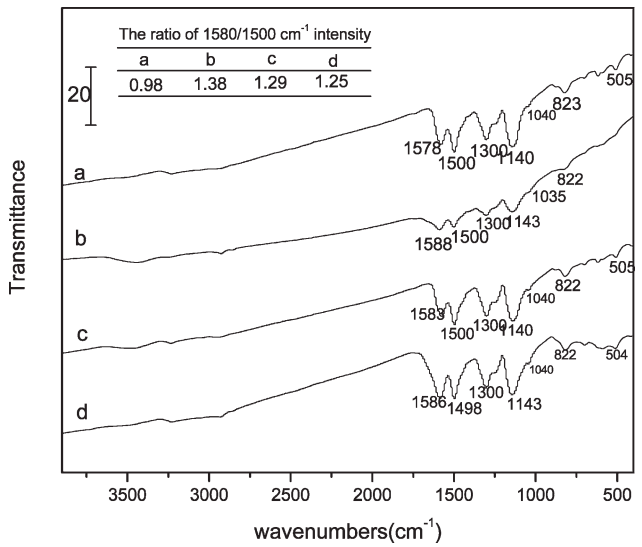

Figure 5 Infrared spectra of PANI with $[NiCl_2]/[Ani]$ molar ratios of (a) 0, (b) 0.5, (c) 1.0, and (d) 2.0.

1140 cm^{-1} related to proton doping PANI, and the out-of-plane deformation of C—H bond in 1,4-disubstituted benzene ring at 822 cm^{-1}[1,18] were clearly observed; this demonstrated that the products were distinct structures of PANI. In particular, shoulder peaks around 1041 and 505 cm^{-1}, ascribed to the absorption of the $-SO_3H$ group,[17] were observed; this demonstrated that the PANI was doped with D-CSA. According to the results of the inset table in Figure 5, the ratio at about 1580/1500 cm^{-1} intensity in PANI, that is, the ratio of quinoid rings to benzoid rings in the molecules of PANI,[24] increased when the molar ratio of $[Ni^{2+}]$ to [Ani] was 0.5, whereas the ratio decreased with increasing of Ni^{2+} from 0.5 to 2.0. MacDiarmid et al.,[25] for the first time, proposed that proton doping only took place on the imine segment. Thus, we speculated that the combination between Ni^{2+} and SO_3^- in CSA led to a reduction in CSA doping to PANI at a small amount of loading of Ni^{2+}; this resulted in a decrease in the doping degree. The higher loading of Ni^{2+} may have been brought about by direct doping by Ni^{2+}, which induced a higher degree of doping.

To confirm that Ni^{2+} was doped into the molecules of PANI, elemental analysis with ICP–AES was performed, and the results are summarized in Table I. The amount of Ni^{2+} ions present in the resulting PANI was found to increase with increasing molar ratio of $[NiCl_2]$ to [Ani] in the polymerization system. The results illustrate that the transition-metal ion, Ni^{2+}, was successfully incorporated into the polymeric chain and caused a higher doping degree of PANI, which agreed well with the FTIR analysis (Fig. 5).

Figure 6 shows the UV–vis absorption spectra of D-CSA-doped and CSA–$NiCl_2$-codoped PANI. For the D-CSA-doped PANI, the absorption peak at

TABLE I
Characteristics of the PANI Prepared in This Study

Sample number	$[NiCl_2]/[Ani]$ molar ratio[a]	Nickel content in the sample (wt %)	Room-temperature conductivity (S/cm)
1	0	0	0.232
2	0.5	0.37	0.453
3	1.0	0.56	0.926
4	2.0	0.87	1.727

[a] The [CSA]/[Ani] and [APS]/[Ani] molar ratios were kept at 0.5 and 1.0, respectively, in the reaction media.

359 nm was assigned to the π–π* transition of the benzenoid ring,[26] and the band located at 614 nm was attributed to the benzenoid-to-quinoid excitonic transition.[27] Upon protonation by doping with D-CSA and Ni^{2+}, the intensity of the excitonic transition gradually decreased but did not disappear; this indicated that the resulting PANI was partially protonated. In comparison, the CSA–$NiCl_2$ codoped samples [Fig. 6(b–d)] corresponding to about 351 and 576 nm displayed blueshifts of 8 and 38 nm, respectively. This phenomenon could be explained by interactions between the D-CSA molecules and Ni^{2+}, which influenced the molecular configuration and band structure of PANI. Ni^{2+} doped onto PANI increased the intermolecular interaction and widened the energy band gap; this led to a blueshift of the π–π* transition. In addition, the interaction between Ni^{2+} and CSA might have influenced the doping degree.

Figure 7 shows the XRD patterns of PANI without $NiCl_2$ and with $NiCl_2$ at different $[NiCl_2]/[Ani]$ molar ratios. The sharp peak centered at $2\theta = 6.5°$ was assigned to the periodicity distance between the dopant and N atom on adjacent main chains, and

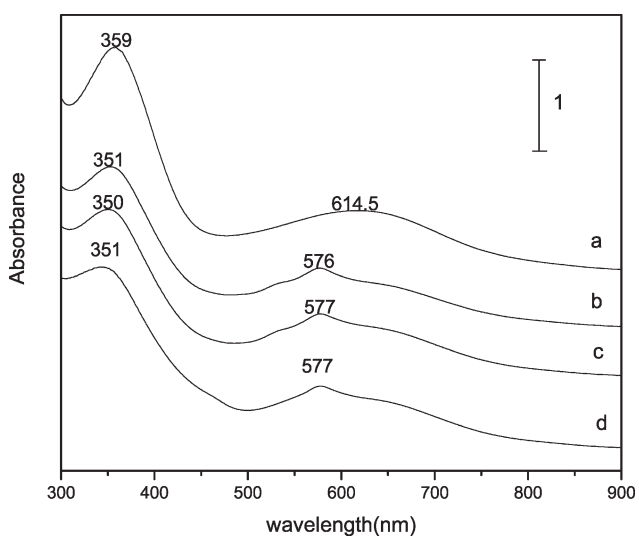

Figure 6 UV–vis spectra of PANI under $[NiCl_2]/[Ani]$ molar ratios of (a) 0, (b) 0.5, (c) 1.0, and (d) 2.0.

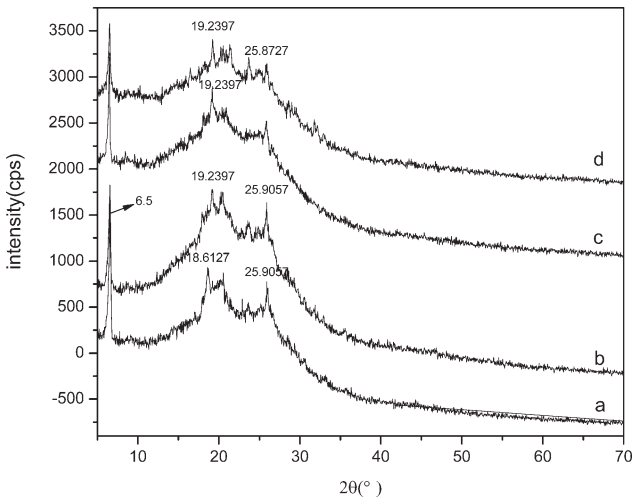

Figure 7 XRD patterns of PANI under $[NiCl_2]/[Ani]$ molar ratios of (a) 0, (b) 0.5, (c) 1.0, and (d) 2.0.

the later broad bands centered at about $2\theta = 18.6$ and 25.9° were ascribed to the periodicities parallel and perpendicular to the polymer chains of PANI, respectively.[28] For the Ni^{2+}-codoped samples, the peak for denoting the periodicity parallel to the polymer chains of PANI[29] shifted from $2\theta = 18.6$ to 19.2°, and the intensity of the two broad peaks centered at $2\theta = 19.2$ and 25.9° decreased. This indicated that the addition of Ni^{2+} may have led to a decrease in the orientation of the molecules.

Conductivity

The room-temperature conductivities of CSA-doped and CSA–Ni^{2+}-codoped PANI are summarized in Figure 8. The conductivity increased with the increasing Ni^{2+} loading. Generally, the room-temperature conductivity of a polymer mainly depends on the doping degree. According to the results of FTIR spectroscopy

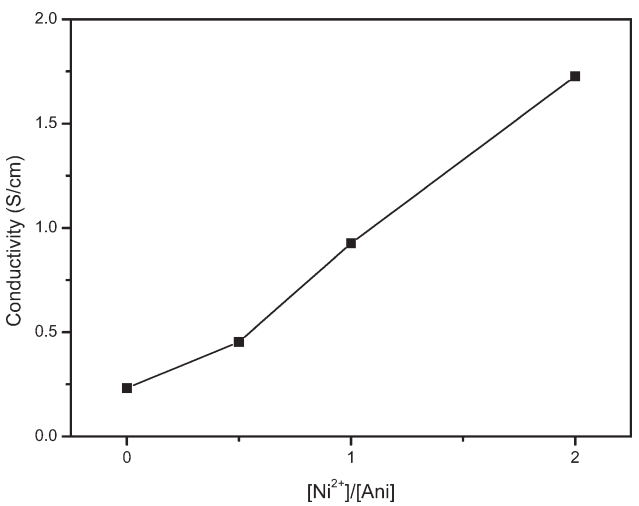

Figure 8 Effect of Ni^{2+} loading on the conductivity of CSA–Ni^{2+} codoped PANI.

(Fig. 5), the ratio of quinoid rings to benzoid rings in the molecules of PANI decreased with increasing $[Ni^{2+}]/[Ani]$ molar ratio from 0.5 to 2.0; this indicated that more Ni^{2+} doping took place on the imine segment to form charge carriers. Thus, it demonstrated the higher degree of doping in the higher loading of Ni^{2+}. The results of ICP–AES analysis also indicated that the Ni^{2+} brought about direct doping to PANI and increased the doping degree. As a comprehensive consideration of the results of the structural characterization and the mechanism analyses, we attributed this phenomenon to the effective doping of Ni^{2+} to the PANI molecules.

CONCLUSIONS

In summary, 1-D nanostructures of PANI doped with D-CSA alone and with Ni^{2+} as a codopant were successfully synthesized via *in situ* polymerization. The ICP–AES analysis and FTIR spectra illustrated that the transition-metal ion, Ni^{2+}, was successfully incorporated into the polymeric chain. SEM images showed that PANI–CSA–Ni^{2+} with different $[NiCl_2]/[Ani]$ molar ratios exhibited greatly different structures from PANI–CSA because the micelles composed of D-CSA anions and anilinium cations were destroyed by the Ni^{2+} addition. We also found that a small amount of Ni^{2+} led to a reduction in the doping degree of CSA to PANI, and a higher loading of Ni^{2+} might have brought about the direct doping to PANI by Ni^{2+}. This induced a higher degree of doping and a higher conductivity of the nanostructured PANI.

References

1. Skotheim, T. A.; Elsenbaumer, R. L.; Reynolds, J. R. Handbook of Conducting Polymers, 2nd ed.; Marcel Dekker: New York, 1998.
2. Zhao, D. L.; Li, X.; Shen, Z. M. J Alloys Compd 2009, 471, 457.
3. Cheng, Q. L.; He, Y.; Pavlinek, V.; Li, C. Z.; Saha, P. Synth Met 2008, 158, 953.
4. Chang, M. Y.; Wu, C. S.; Chen, Y. F.; Hsieh, B. Z.; Huang, W. Y.; Ho, K. S.; Hsiehband, T. S.; Han, Y. K. Org Electron 2008, 9, 1136.
5. Sutar, D. S.; Padma, N.; Aswal, D. K. H. Sens Actuators B 2007, 128, 286.
6. Liu, F. J.; Huang, L. M.; Wen, T. C.; Gopalan, A.; Hung, J. S. Mater Lett 2007, 61, 4400.
7. Wang, X. H.; Shao, M. W.; Shao, G.; Wu, Z. C.; Wang, S. W. J Colloid Interface Sci 2009, 332, 74.
8. Kong, L. R.; Lu, X. F.; Jin, E.; Jiang, S.; Wang, C.; Zhang, W. J. Compos Sci Technol 2009, 69, 561.
9. He, Q.; Cui, Y.; Ai, S. F.; Tian, Y.; Li, J. B. Curr Opin Colloid Interface Sci 2009, 14, 115.
10. Zhang, Z. M.; Wei, Z. X.; Zhang, L. J.; Wan, M. X. Acta Mater 2005, 53, 1373.
11. Sengupta, P. P.; Kar, P.; Adhikari, B. React Funct Polym 2008, 68, 1103.
12. Tang, Q. W.; Sun, X. M.; Li, Q. H.; Wu, J. H.; Lin, J. M.; Huang, M. L. Mater Lett 2009, 63, 540.
13. Zhang, Z. M.; Deng, J. Y.; Yu, L. M.; Wan, M. X. Synth Met 2008, 158, 712.
14. Yang, C. M.; Chen, C. Y. Synth Met 2005, 153, 133.

15. Dimitriev, O. P. Synth Met 2004, 142, 299.
16. Chen, S. N.; Lin, L. C. Macromolecules 1995, 28, 1239.
17. Zhang, L. J.; Wan, M. X. Nanotechnology 2002, 13, 750.
18. Hatchett, D. W.; Josowicz, M.; Janata, J. J Electrochem Soc 1999, 146, 4535.
19. Sevil, U. A.; Guven, O.; Suzer, S. J Phys Chem B 1998, 102, 3902.
20. Conwell, E.; Duke, C. B.; Paton, A.; Leyadev, S. J. J Chem Phys 1988, 88, 3955.
21. Furudawa, Y.; Ueda, F.; Hyodo, Y.; Harada, I.; Nakajima, T.; Kawagoe, T. Macromolecules 1988, 21, 1297.
22. Lu, J. X.; Moon, K. S.; Kim, B. K.; Wong, C. P. Polymer 2007, 48, 1510.
23. Gao, H. X.; Jiang, T.; Han, B. X.; Wang, Y.; Du, J. M.; Liu, Z. M.; Zhang, J. L. Polymer 2004, 45, 3017.
24. Zengin, H.; Zhou, W. S.; Jin, J. Y.; Czerw, R.; Smith, D. W., Jr.; Echegoyen, L.; Carroll, D. L.; Foulger, S. H.; Ballato, J. Adv Mater 2002, 14, 1480.
25. Huang, W. S.; Humphrey, B. D.; MacDiarmid, A. G. J Chem Soc Faraday Trans 1986, 82, 2385.
26. Epstein, A. J.; Ginder, J. M.; Zuo, F.; Bigelow, R. W.; Woo, H. S.; Tanner, D. B.; Richter, A. F.; Huang, W. S.; MacDiarmid, A. G. Synth Met 1987, 21, 63.
27. Venugopal, G.; Quan, X.; Johnson, G. E.; Houlihan, F. M.; Chin, E.; Nalamasu, O. Chem Mater 1995, 7, 271.
28. Zhang, L.; Zhang, L. J.; Wan, M. X.; Wei, Y. Synth Met 2006, 156, 454.
29. Yang, Y. S.; Wan, M. X. Mater Chem 2002, 12, 897.